Chapter 9
A Review on Self-oscillating Relay Feedback Systems and Its Application to Underactuated Systems with Degree of Underactuation One

Luis T. Aguilar, Igor Boiko, Leonid Fridman, and Rafael Iriarte

Abstract. A tool for the design of a periodic motion in underactuated systems via generating a self-excited oscillation of a desired amplitude and frequency driven by a variable structure control is reviewed. In this chapter, we overview the capabilities of the two-relay controller to induce oscillations in dynamical systems. In this chapter, we will focus on underactuated mechanical systems with degree of underactuation one, that is, n degrees-of-freedom and $n-1$ actuators only. Three methods to set the frequency and amplitude of oscillation and its application to one-degree of underactuation systems are reviewed: describing function method, Locus of the perturbed relay system design (LPRS), and Poincaré map based design. Theoretical and practical open problems are also discussed.

9.1 Introduction

Researchers have been investigating and applying limit cycle behaviour to many different engineering fields. We can find several research works on this subject (see, e.g., [26]) but in the present survey we will focus on limit cycles induced by relay feedback systems only. In this chapter, we review the control of one of the simplest

Luis T. Aguilar · Rafael Iriarte
Instituto Politécnico Nacional, Ave. del parque 1310 Mesa de Otay,
Tijuana Baja California 22510
e-mail: {laguilar,ririarte}@citedi.mx

Igor Boiko
Electrical Engineering Department, The Petroleum Institute,
P.O. BOX 2533, Abu Dhabi, U.A.E.
e-mail: i.boiko@ieee.org

Leonid Fridman
Universidad Nacional Autónoma de México Departamento de Ingeniería de Control,
UNAM, México, D.F., 04510
e-mail: lfridman@unam.mx

B. Bandyopadhyay et al. (Eds.): *Advances in Sliding Mode Control*, LNCIS 440, pp. 187–205.
DOI: 10.1007/978-3-642-36986-5_9

types of functional motion: generation of a periodic motion in underactuated systems which could be non-minimum-phase. Current representative works on periodic motions and orbital stabilization of underactuated systems involve finding and using a reference model as a generator of limit cycles (see, e.g., [9, 25]), thus considering the problem of obtaining a periodic motion as a servo problem. Orbital stabilization of underactuated systems finds applications in electrical and mechanical systems.

Electrical systems. In power electronics applications, the idea of using self-oscillating switching has been explored in dc–dc inverters [22] because zero sensitivity to load changes and high performance have been demonstrated. Such inverters are attractive to operate in dc–ac converters since two buck-boost dc–dc inverters are commonly used. Several topologies have been proposed to design these converters, for example, Sanchis *et al*. [27] design a buck-boost dc–ac inverter using a double-loop control for both buck-boost dc–dc converter. Youssef and Jain [32] present a self-sustained oscillating controller for power factor correction circuits. Several circuit topologies for nonconventional dc–ac inverters are illustrated in J. Lai [19]. Under the framework of the present chapter, the dc–ac converter will consists of a two relay controller and a second order filter. For example, in an uninterruptible power supply (UPS) units, the desired voltage and frequency will be taken as 120 V_{rms} and 60 Hz, respectively according to North America standard. Thus, the purpose of the two relay controller is to induce a periodic voltage at the output of the filter with desired frequency and amplitude avoiding fast switching.

Underactuated mechanical systems. In particular, one of the most interesting applications of self-oscillation is to develop motion-planning algorithms which allow an underactuated robot to execute reliable maneuvers which is still a challenge for this class of systems for example in the coordinated motion of biped robots [12]. The formulation is different from the typical formulation of the tracking control problem for fully actuated mechanical systems [30] where the reference trajectory can be arbitrarily given, because underactuated systems are not feedback linearizables due to the insufficient number of actuators. Therefore, special attention is required in the selection of the desired trajectory for the systems under study. Different approaches for orbital stabilization have been proposed. For example, Shiriaev *et al*. [29] introduces a constructive tool for generation and orbital stabilization of periodic motion in underactuated nonlinear system through virtual constraint approach. Grizzle *et al*. [18] demonstrate asymptotic tracking for an unactuated link by finding conditions for the existence of a set of outputs that yields a system with a one-dimensional exponentially stable zero dynamics. In Orlov *et al*. [24] and Santiesteban *et al*. [28] an asymptotic harmonic generator was introduced through a modified Van der Pol equation tested on a friction pendulum to solve the swing up problem for an inverted pendulum. Berkemeier and Fearing [9] derive a set of exact trajectories of the nonlinear equations of motion of Acrobot, which involve inverted periodic motions. Martínez *et al*. [21] made a study of motion planning and oscillatory control for underactuated systems under geometric control theory.

In this chapter, underactuated systems are considered as the systems with internal (unactuated) dynamics with respect to the actuated variables. It allows us to propose

a method of generating a periodic motion in an underactuated system where the same behavior can be seen via second order sliding mode (SOSM) algorithms, that is, generating self-excited oscillations using the same mechanism as the one that produces chattering. However, the generalization of the SOSM algorithms and the treatment of the unactuated part of the plant as additional dynamics result in the oscillations that may not necessarily be fast and of small amplitude.

There exist two approaches to analysis of periodic motions in sliding mode systems due to the presence of additional dynamics: the time-domain approach, which is based on the state space representation, and the frequency-domain approach. The Poincaré maps [31] are successfully used to ensure the existence and stability of periodic motions in the relay control systems (see, e.g., [16]). We can find application of Poincaré maps in several tasks such as biped locomotion [23] and switched converter systems [13]. The describing function (DF) method [15] allows approximate values of the frequency and the amplitude of periodic motions to be found in systems with linear plants driven by sliding mode controllers. The locus of perturbed relay system (LPRS) method [10] provides an exact solution of the periodic problem in discontinuous control systems, including finding exact values of the amplitude and the frequency of the self-excited oscillation.

Biped robots, gymnastic robot, and mechanical systems that evolve coordinated motion in order to emulate human walking patterns and climbing are examples of slow motion systems while switching power supplies are examples where fast oscillations are required. In this chapter, we will focus in underactuated mechanical systems with degree of underactuation one, that is, n degrees-of-freedom and $n-1$ actuators. Examples of such systems are inertia wheel pendulum, acrobot, pendubot, among others.

9.2 Problem Statement

Let the underactuated mechanical system, which is a plant in the system where a periodic motion is supposed to occur, be given by the Lagrange equation:

$$M(q)\ddot{q} + H(q,\dot{q}) = Su \tag{9.1}$$

where $q(t) \in \mathbb{R}^m$ is the vector of joint positions; $u(t) \in \mathbb{R}$ is the vector of applied joint torques where $m < n$; $S = [0_{(m-1)}, 1]^T$ is the input that maps the torque input to the joint coordinates space; $M(q) \in \mathbb{R}^{m\times m}$ is the symmetric positive-definite inertia matrix; and $H(q,\dot{q}) \in \mathbb{R}^m$ is the vector that contains the Coriolis, centrifugal, gravity, and friction torques.

The following two-relay controller is proposed for the purpose of exciting a periodic motion:

$$u = -c_1 \operatorname{sign}(y) - c_2 \operatorname{sign}(\dot{y}), \tag{9.2}$$

where c_1 and c_2 are parameters designed such that the scalar output of the system (the position of a selected link of the plant)

$$y = h(q) \tag{9.3}$$

has a steady periodic motion with the desired frequency and amplitude.

The *analysis and design objectives* are formulated as follows: Find the parameter values c_1 and c_2 in (9.2) such that the system (9.1) has a periodic motion with the desired frequency Ω and desired amplitude of the output signal A_1. Therefore, the main objective of this research is to find mapping G to be able to tune c_1 and c_2 values.

9.3 Methodologies Review

In Aguilar *et al.* [5, 6] was demonstrated the capabilities of the two relay controller to induce oscillations in nonlinear dynamical systems. Indeed, due to the simplicity of the controller to solve such problem, it looks attractive for its physical implementation. The TRC were successfully tested in academic underactuated systems (inverted pendulums). However, we can found in literature many underactuated systems with certain degree of complexity where motion control is required. Analysis of periodic motions in variable structure system were studied by Fridman [17]. The introductory works [2–4] were motivated by the original works of Boiko and Fridman compiled in [11] where the analysis of chattering in linear systems was pursued using frequency domain tools such as describing function and locus of a perturbed relay systems (LPRS) methods.

9.3.1 Describing Function

Let firstly, the linearized plant be given by:

$$\begin{array}{l} \dot{x} = Ax + Bu \\ y = Cx \end{array}, \qquad x \in \mathbb{R}^n, \quad y \in \mathbb{R}, \quad n = 2m \tag{9.4}$$

which can be represented in the transfer function form as follows:

$$W(s) = C(sI - A)^{-1}B.$$

Let us assume that matrix A has no eigenvalues at the imaginary axis and the relative degree of (9.4) is greater than 1.

The describing function (DF), N, of the variable structure controller (9.2) is the first harmonic of the periodic control signal divided by the amplitude of $y(t)$ [8]:

$$N = \frac{\omega}{\pi A_1}\int_0^{2\pi/\omega} u(t)\sin(\omega t)dt + j\frac{\omega}{\pi A_1}\int_0^{2\pi/\omega} u(t)\cos(\omega t)dt \tag{9.5}$$

where A_1 is the amplitude of the input to the nonlinearity (of $y(t)$ in our case) and ω is the frequency of $y(t)$. However, the algorithm (9.2) can be analyzed as the parallel

connection of two ideal relay where the input to the first relay is the output variable and the input to the second relay is the derivative of the output variable. For the first relay the DF is:

$$N_1 = \frac{4c_1}{\pi A_1},$$

and for the second relay it is [[8]]:

$$N_2 = \frac{4c_2}{\pi A_2},$$

where A_2 is the amplitude of dy/dt. Also, take into account the relationship between y and dy/dt in the Laplace domain, which gives the relationship between the amplitudes A_1 and A_2: $A_2 = A_1\Omega$, where Ω is the frequency of the oscillation. Using the notation of the algorithm (9.2) we can rewrite this equation as follows:

$$N = N_1 + sN_2 = \frac{4c_1}{\pi A_1} + j\Omega\frac{4c_2}{\pi A_2} = \frac{4}{\pi A_1}(c_1 + jc_2), \tag{9.6}$$

where $s = j\Omega$. Let us note that the DF of the algorithm (9.2) depends on the amplitude value only. This suggests the technique of finding the parameters of the limit cycle via the solution of the harmonic balance equation [[8]]:

$$W(j\Omega)N(a) = -1, \tag{9.7}$$

where a is the generic amplitude of the oscillation at the input to the nonlinearity, and $W(j\omega)$ is the complex frequency response characteristic (Nyquist plot) of the plant. Using the notation of the algorithm (9.2) and replacing the generic amplitude with the amplitude of the oscillation of the input to the first relay this equation can be rewritten as follows:

$$W(j\Omega) = -\frac{1}{N(A_1)}, \tag{9.8}$$

where the function at the right-hand side is given by:

$$-\frac{1}{N(A_1)} = \pi A_1\frac{-c_1 + jc_2}{4(c_1^2 + c_2^2)}.$$

Equation (9.7) is equivalent to the condition of the complex frequency response characteristic of the open-loop system intersecting the real axis in the point $(-1, j0)$. The function $-1/N$ is a straight line the slope of which depends on c_2/c_1 ratio. The point of intersection of this function and of the Nyquist plot $W(j\omega)$ provides the solution of the periodic problem.

Here, we summarize the steps to tune c_1 and c_2:

a) Identify the quadrant in the Nyquist plot where the desired frequency Ω is located, which falls into one of the following categories (sets):

$$Q_1 = \{\omega \in \mathbb{R} : \mathrm{Re}\{W(j\omega)\} > 0, \mathrm{Im}\{W(j\omega)\} \geq 0\}$$
$$Q_2 = \{\omega \in \mathbb{R} : \mathrm{Re}\{W(j\omega)\} \leq 0, \mathrm{Im}\{W(j\omega)\} \geq 0\}$$
$$Q_3 = \{\omega \in \mathbb{R} : \mathrm{Re}\{W(j\omega)\} \leq 0, \mathrm{Im}\{W(j\omega)\} < 0\}$$
$$Q_4 = \{\omega \in \mathbb{R} : \mathrm{Re}\{W(j\omega)\} > 0, \mathrm{Im}\{W(j\omega)\} < 0\}.$$

b) The frequency of the oscillations depends only on the c_2/c_1 ratio, and it is possible to obtain the desired frequency Ω by tuning the $\xi = c_2/c_1$ ratio:

$$\xi = \frac{c_2}{c_1} = -\frac{\mathrm{Im}\{W(j\Omega)\}}{\mathrm{Re}\{W(j\Omega)\}}. \tag{9.9}$$

Since the amplitude of the oscillations is given by

$$A_1 = \frac{4}{\pi}|W(j\Omega)|\sqrt{c_1^2 + c_2^2}, \tag{9.10}$$

then the c_1 and c_2 values can be computed as follows

$$c_1 = \begin{cases} \frac{\pi}{4}\frac{A_1}{|W(j\Omega)|}\left(\sqrt{1+\xi^2}\right)^{-1} & \text{if } \Omega \in Q_2 \cup Q_3 \\ -\frac{\pi}{4}\frac{A_1}{|W(j\Omega)|}\left(\sqrt{1+\xi^2}\right)^{-1} & \text{elsewhere} \end{cases} \tag{9.11}$$

$$c_2 = \xi \cdot c_1. \tag{9.12}$$

9.3.2 Locus of a Perturbed Relay System Design (LPRS)

The LPRS proposed in [[10]] provides an exact solution of the periodic problem in a relay feedback system having a plant (9.4) and the control given by the hysteretic relay. The LPRS is defined as a characteristic of the response of a linear part to an unequally spaced pulse control of variable frequency in a closed-loop system [[10]]. This method requires a computational effort but will provide an exact solution. The LPRS can be computed as follows:

$$J(\omega) = \sum_{k=1}^{\infty}(-1)^{k+1}\mathrm{Re}\{W(k\omega)\} + j\sum_{k=1}^{\infty}\frac{1}{2k-1}\mathrm{Im}\{W[(2k-1)\omega]\}. \tag{9.13}$$

The frequency of the periodic motion for the algorithm (9.2) can be found from the following equation [[10]]:

$$\mathrm{Im}J(\Omega) = 0.$$

In fact, we are going to consider the plant being nonlinear, with the second relay transposed to the feedback in this equivalent plant. Introduce the following function, which will be instrumental in finding a response of the nonlinear plant to the periodic square-wave pulse control.

$$L(\omega,\theta)=\sum_{k=1}^{\infty}\frac{1}{2k-1}(\sin[(2k-1)2\pi\theta]\mathrm{Re}\{W[(2k-1)\omega]\} + \cos[(2k-1)2\pi\theta]\mathrm{Im}\{W[(2k-1)\omega]\}). \tag{9.14}$$

The function $L(\omega,\theta)$ denotes a linear plant output (with a coefficient) at the instant $t=\theta T$ (with T being the period: $T=2\pi/\omega$) if a periodic square-wave pulse signal of unity amplitude is applied to the plant:

$$L(\omega,\theta)=\left.\frac{\pi y(t)}{4c}\right|_{t=2\pi\theta/\omega}$$

with $\theta\in[-0.5,0.5]$ and $\omega\in[0,\infty]$, where $t=0$ corresponds to the control switch from -1 to $+1$.

With $L(\omega,\theta)$ available, we obtain the following expression for $\mathrm{Im}\{J(\omega)\}$ of the equivalent plant:

$$\mathrm{Im}\{J(\omega)\}=L(\omega,0)+\frac{c_2}{c_1}L(\omega,\theta). \tag{9.15}$$

The value of the time shift θ between the switching of the first and second relay can be found from the following equation

$$\dot{y}(\theta)=0.$$

As a result, the set of equations for finding the frequency Ω and the time shift θ is as follows:

$$c_1L(\Omega,0)+c_2L(\Omega,\theta)=0,\quad c_1L_1(\Omega,-\theta)+c_2L_1(\Omega,0)=0. \tag{9.16}$$

The amplitude of the oscillations can be found as follows. The output of the system is:

$$y(t)=\frac{4}{\pi}\sum_{i=1}^{\infty}\{c_1\sin[(2k-1)\Omega+\varphi_L((2k-1)\Omega)] + c_2\sin[(2k-1)\Omega t+\varphi_L((2k-1)\Omega)+(2k-1)2\pi\theta]\}A_L((2k-1)\Omega) \tag{9.17}$$

where $\varphi_L(\omega)=argW(\omega)$, which is a response of the plant to the two square pulse-wave signals shifted with respect to each other by the angle $2\pi\theta$. Therefore, the amplitude is

$$A_1=\max_{t\in[0;2\pi/\omega]}y(t). \tag{9.18}$$

Yet, instead of the true amplitude we can use the amplitude of the fundamental frequency component (first harmonic) as a relatively precise estimate. In this case, we can represent the input as the sum of two rotating vectors having amplitudes $4c_1/\pi$ and $4c_2/\pi$, with the angle between the vectors $2\pi\theta$. Therefore, the amplitude of the control signal (first harmonic) is

$$A_u = \frac{4}{\pi}\sqrt{c_1^2 + c_2^2 + 2c_1c_2\cos(2\pi\theta)}, \tag{9.19}$$

and the amplitude of the output (first harmonic) is

$$A_1 = \frac{4}{\pi}\sqrt{c_1^2 + c_2^2 + 2c_1c_2\cos(2\pi\theta)}A_L(\Omega), \tag{9.20}$$

where $A_L(\omega) = |W(j\omega)|$. We should note that despite using approximate value for the amplitude in (9.20), the value of the frequency is exact. Expressions (9.16), (9.20) if considered as equations for Ω and A_1 provide one with mapping F. From (9.16) one can see that the frequency of the oscillations depends only on the ratio $c_2/c_1 = \xi$. Therefore, Ω is invariant with respect to c_2/c_1: $\Omega(\lambda c_1, \lambda c_2) = \Omega(c_1, c_2)$. It also follows from (9.20) that there is the following invariance for the amplitude: $A_1(\lambda c_1, \lambda c_2) = \lambda A_1(c_1, c_2)$. Therefore, Ω and A_1 can be manipulated independently in accordance with mapping G considered below.

Mapping G (inverse of F) can be derived from (9.16), (9.20) if c_1, c_2 and θ are considered unknown parameters in those equations. For any given Ω, from equation (9.16) the ratio $c_2/c_1 = \xi$ can be found (as well as θ). Therefore, we can find first $\xi = c_2/c_1 = h(\Omega)$, where $h(\Omega)$ is an implicit function that corresponds to (9.16). After that c_1 and c_2 can be computed as per the following formulas:

$$c_1 = \frac{\pi}{4}\frac{A_1}{A_L(\Omega)}\frac{1}{\sqrt{1 + 2\xi\cos(2\pi\theta) + \xi^2}} \tag{9.21}$$

$$c_2 = \frac{\pi}{4}\frac{A_1}{A_L(\Omega)}\frac{\xi}{\sqrt{1 + 2\xi\cos(2\pi\theta) + \xi^2}}. \tag{9.22}$$

9.3.3 Poincaré-Map-Based Design

To construct the Poincaré map, one has to choose a surface of section S in the state space $\mathbb{R}^4$ and consider the points of successive intersections of a given trajectory with this surface. Switching occur on the level surfaces defined by

$$\begin{aligned} S_1 &= \{x : y = 0, \dot{y} < 0\}, & S_2 &= \{x : y < 0, \dot{y} = 0\}, \\ S_3 &= \{x : y = 0, \dot{y} > 0\}, & S_4 &= \{x : y > 0, \dot{y} = 0\}. \end{aligned} \tag{9.23}$$

The space $\mathbb{R}^4$ is divided into four regions by S_i, $i = 1, \ldots, 4$:

$$\begin{aligned} R_1 &= \{x : y < 0, \dot{y} < 0\}, & R_2 &= \{x : y < 0, \dot{y} > 0\}, \\ R_3 &= \{x : y > 0, \dot{y} > 0\}, & R_4 &= \{x : y > 0, \dot{y} < 0\}. \end{aligned} \tag{9.24}$$

Depending on the state, the system is governed by one of the four models defined by

$$
\begin{aligned}
M_1 &: \dot{x} = Ax + B(c_1 + c_2),\\
M_2 &: \dot{x} = Ax + B(c_1 - c_2),\\
M_3 &: \dot{x} = Ax - B(c_1 + c_2),\\
M_4 &: \dot{x} = Ax + B(-c_1 + c_2).
\end{aligned}
$$

The solution of M_1 on the time interval $[0;t_1]$, where t_1 is the transition time from S_1 to S_2, subject to the initial conditions $x(0) = \rho_p$, where "$(\cdot)_p$" stands for "periodic", such that (without loss of generality)

$$
\begin{aligned}
y(0) = Cx(0) = C\rho_p = 0,\\
\dot{y}(0) = C(Ax(0) + Bu) = CA\rho_p < 0
\end{aligned}
\tag{9.25}
$$

is given by

$$
x(t) = e^{At}x(0) + \int_0^t e^{A\tau}d\tau Bu,
$$

where

$$
\int_0^t e^{A\tau}d\tau = \sum_{i=1}^{\infty} A^{i-1}t^i/i! = A^{-1}(e^{At} - I)
$$

and $u = c_1 + c_2$. The transition to S_2 and switching to $u = c_1 - c_2$ is ensured under the technical transversality condition

$$
\ddot{y}(t_1) = CA^2\eta_k > 0. \tag{9.26}
$$

Under this condition, the trajectory will enter the region R_2, and since the matrix A is Hurwitz it will reach either S_3 or return back to S_2. We will assume for now that the latter does not happen.

Analogously, for the case of the twisting projection of the motion onto the $(y,\dot{y})$-plane, the four state transitions initiated at $\rho_k = \rho_p$ are given by

$$
\begin{aligned}
\eta_k &= e^{At_1}\rho_k + A^{-1}(e^{At_1} - I)B(c_1 + c_2),\\
\rho_k^- &= e^{At_2}\eta_k + A^{-1}(e^{At_2} - I)B(c_1 - c_2),\\
\eta_k^- &= e^{At_3}\rho_k^- - A^{-1}(e^{At_3} - I)B(c_1 + c_2),\\
\rho_{k+1} &= e^{At_4}\eta_k^- - A^{-1}(e^{At_4} - I)B(c_1 - c_2),
\end{aligned}
\tag{9.27}
$$

where t_2 is the time interval between S_2 and S_3, t_3 is the time interval between S_3 and S_4, and t_4 is the time interval between S_4 and S_1.

The fixed point of the Poincaré map, corresponding to an isolated periodic solution of system (9.4) driven by the two-relay controller, is determined by equation $\rho_{k+1} = \rho_k = \rho_p$. Skipping the sequential numbers of switching in (9.27) and using the principle of symmetry one can write the following: $\rho_p^- = -\rho_p$. For the T-periodic (symmetric) solution we will use the following notation: $t_1 = t_3 = \theta_1$, $t_2 = t_4 = \theta_2 = T/2 - \theta_1$.

The equation for the fixed point together with the switching conditions can be rewritten as follows:

$$-\rho_p = e^{A\theta_2}\eta_p + A^{-1}(e^{A\theta_2} - I)B(c_1 - c_2) \tag{9.28}$$

and, with the help of $y(0) = \dot{y}(\theta_1) = 0$ and $CB = 0$,

$$\begin{gathered} \eta_p = e^{A\theta_1}\rho_p + A^{-1}(e^{A\theta_1} - I)B(c_1 + c_2) \\ C\rho_p = 0, \quad CA\eta_p = 0, \quad CA\rho_p < 0, \quad CA^2\eta_p > 0. \end{gathered} \tag{9.29}$$

We assume in (9.28) and (9.29) that there are no additional switches on intervals $t \in (0;t_1)$ and $t \in (t_1;t_2)$, respectively since $\dot{y} < 0$ initially and y monotonically decreases from zero and cannot cross zero before $\dot{y}$ changes sign at $t = t_1$. This condition can easily be verified after parameters θ_1 and θ_2 are determined.

It is left to formalize the condition ensuring transition from S_2 to S_3 without leaving R_2. Defining two hypothetical (for the fixed control input $u = c_1 - c_2$) boundary crossing times as $\bar{t}_2$ and t_2, we have

$$t_2 = \min\left\{t > 0 : C\left(e^{At}\eta_p + A^{-1}(e^{At} - I)B(c_1 - c_2)\right) = 0\right\}$$

and

$$\bar{t}_2 = \min\left\{t > 0 : CA\left(e^{At}\eta_p + A^{-1}(e^{At} - I)B(c_1 - c_2)\right) = 0\right\}.$$

Hence, we require

$$t_2 < \bar{t}_2 \tag{9.30}$$

to ensure that our analysis of the limit cycle with exactly four switches is correct. In the case when the transition time is sufficiently small, dropping smaller-order terms in the definitions of t_2 and $\bar{t}_2$, one can derive the following simplified approximate algebraic assumption[1]

$$0 < t_2 \approx -\frac{2CA^2\eta_p}{CA^3\eta_p + c_2 - c_1} < \sqrt{\frac{2C\eta_p}{-CA^2\eta_p}} \approx \bar{t}_2.$$

Let us move onto defining the amplitude and frequency of the oscillations.

The system (9.28) and (9.29) can be considered as a system of algebraic equations for design of the two-relay controller providing for the system (9.4) the desired periodic solution with a given frequency Ω and amplitude A_1. Taking into account that

$$y(\theta_1) = C\eta_p = A_1, \quad \theta_1 + \theta_2 = \pi/\Omega = T/2 \tag{9.31}$$

(9.28), (9.29), and (9.31) can be reduced to a system of five nonlinear algebraic equations with respect to five variables: c_1, c_2, θ_1 and the first and the second coordinates of the vector ρ_p. Once the resolving set of parameters is found, the two-relay controller gains that provide the periodic solution of the system (9.4) with the desired amplitude and frequency are designed. This can be summarized as follows.

[1] Here we have used the identities $CA\eta_p = 0$, $CB = CAB = 0$, and $CA^2B = 1$, and dropped the third-order terms in the series expansions for the matrix exponents.

Theorem 9.1. *Suppose the system (9.28), (9.29), and (9.31) possesses a solution satisfying (9.30). If the desired amplitude A_1 is sufficiently small to avoid singularity in the matrix $M(q)$ defined in (9.1) and assuming that there are no additional switches on intervals $t \in (0;t_1)$ and $t \in (t_1;t_2)$, then the closed-loop system (9.1)–(9.2) has the desired periodic solution.*

Note however that (9.28), (9.29), and (9.31) is a system of nonlinear algebraic equations and might be hard to solve and even have no solutions for a particular values of A_1 and Ω.

It turns out that the linearity of the (transformed) plant and the fact that the control in the periodic motion can be represented as a sum of two relay controls, with finding the response of the plant as a linear combination (sum) of the two periodic relay controls of amplitudes c_1 and c_2, allows for a reduction of complexity of the original problem. Let us develop an approach that might simplify finding fixed points of the Poincaré map utilizing the concepts of the locus of a perturbed relay system method.

9.4 Linearized-Poincaré-Map-Based Analysis of Orbital Stability

Let us use (9.27) to analyze the deviation of a trajectory initiated on the surface S_1 at $x(0) = \rho_k = \rho_p + \delta_\rho$ from a periodic trajectory initiated from some ρ_p for sufficiently small initial deviations δ_ρ. Using the equation in (9.27) for η_k, the equation in (9.29) for η_p, and the Taylor expansion $e^{At_1} = e^{A\theta_1} + e^{A\theta_1}A\Delta t + O\left(\Delta t^2\right)$, $\Delta t = t_1 - \theta_1$ one can proceed as follows:

$$\begin{aligned}\eta_k &= e^{At_1}(\rho_p + \delta_\rho) + A^{-1}(e^{At_1} - I)B(c_1 + c_2)\\ &= \left(e^{A\theta_1} + e^{A\theta_1}A\Delta t\right)(\rho_p + \delta_\rho) + O\left(\Delta t^2\right)\\ &+ A^{-1}\left(e^{A\theta_1} + (e^{A\theta_1} - I + I)A\Delta t - I\right)B(c_1 + c_2)\end{aligned}$$

so that

$$\eta_k = e^{A\theta_1}\left(\delta_\rho + A\delta_\rho\Delta t\right) + (I + A\Delta t)\eta_p + B(c_1 + c_2)\Delta t + O\left(\Delta t^2\right).$$

Now, since $CA\eta_k = CA\eta_p = 0$, premultiplying this equation by CA which results in

$$CAe^{A\theta_1}\left(\delta_\rho + A\delta_\rho\Delta t\right) + CA(A\eta_p + B(c_1 + c_2))\Delta t = O\left(\Delta t^2\right),$$

one immediately concludes that $\Delta t = O(\delta_\rho)$ and obtains an estimate for $t_1 = \theta_1 + \Delta t$, that can be substituted back:

$$\eta_k = \eta_p + \delta_\eta = \eta_p + \varphi_1\delta_\rho + O(\delta_\rho^2),$$

where

$$\varphi_1 = \left(I - \frac{v_1 CA}{CAv_1}\right) e^{A\theta_1}, \qquad v_1 = A\eta_p + B(c_1 + c_2). \tag{9.32}$$

Following the second equation in (9.27) and computing t_2 using $C\rho_k^- = C\rho_p = 0$, one, in a similar way, obtains

$$\rho_k^- = -\rho_p + \delta_{\rho-} = -\rho_p + \varphi_2 \delta_\eta + O(\delta_\rho^2),$$

where

$$\varphi_2 = \left(I - \frac{v_2 C}{Cv_2}\right) e^{A\theta_2}, \qquad v_2 = A\rho_p + B(c_1 - c_2). \tag{9.33}$$

Following the third equation in (9.27) and computing t_3 using $CA\eta_k^- = CA\eta_p = 0$, one obtains

$$\eta_k^- = -\eta_p + \delta_{\eta-} = -\eta_p + \varphi_3 \delta_{\rho-} + O(\delta_\rho^2),$$

where $\varphi_3 = \varphi_1$.

Following the last equation in (9.27) and computing t_4 using $C\rho_{k+1} = C\rho_p = 0$, one obtains

$$\rho_{k+1} = \rho_p + \varphi_4 \delta_{\rho-} + O(\delta_\rho^2),$$

where $\varphi_4 = \varphi_2$.

Finally, we have for small $\delta_\rho = \rho_k - \rho_p$: $\rho_{k+1} - \rho_p = \Phi \cdot (\rho_k - \rho_p) + O(\delta_\rho^2)$, with

$$\Phi = (\varphi_2 \cdot \varphi_1)^2. \tag{9.34}$$

Since we have just computed a linearization for the Poincaré map, we conclude with the following.

Theorem 9.2. *Suppose that the parameters c_1 and c_2 induce a periodic trajectory for the closed-loop system controlled by the two-relay algorithm, that is, (9.1)–(9.2). This solution is orbitally exponentially stable if and only if all the eigenvalues of the matrix Φ, defined by (9.32), (9.33), and (9.34), are inside the unit circle.*

9.5 Robust Control Design

The system (9.1)–(9.2) is not a free-disturbance system except if there exist a desired frequency and amplitude such that the coefficients of (9.2) satisfy the twisting condition $c_1 > c_2 > w_{\max} > 0$, where $w_{\max}$ is the upper bound of disturbance $w(t)$, that is $\|w(t)\| \leq w_{\max}$. Moreover, the system (9.1) is nonlinear and the design was done considering the linearization of the model, which might result in a closed-loop that is not robust in the presence of unknown inputs. In particular, in Aguilar *et al.* [7], imperfections of oscillation characteristics due to Coulomb friction forces, dead zone, mechanical vibrations, etc., were reported. Motivated by the need of a robust closed-loop scheme, we present a non-autonomous scheme to deal with this problem.

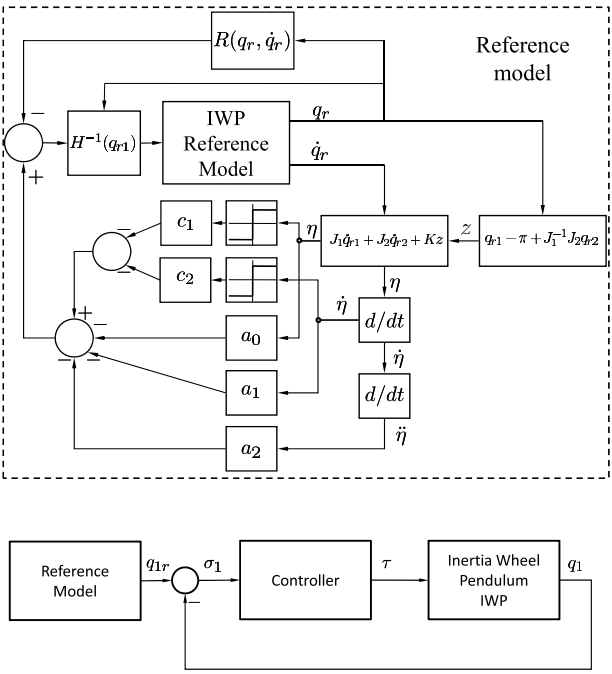

Fig. 9.1 Block diagram of the two-relay controller for real-time trajectory generation for orbital stabilization of inertia wheel pendulum

Let us start by explaining how to find a set of desired oscillations around its upright position. To begin with, let us rewrite (9.1) in terms of the reference positions and velocities $(q_r, \dot{q}_r)$

$$M(q_r)\ddot{q}_r + H(q_r, \dot{q}_r) = Su(y_r, \dot{y}_r). \tag{9.35}$$

We need to find $u(y_r, \dot{y}_r) \in \mathbb{R}$ to produce a set of desired periodic motion of the reference model (y_r) such that its output has a periodic motion with desired frequency and amplitude. Figure 9.1 shows a block diagram of the control applied to the inertia wheel pendulum with the real time trajectory generator.

Finally, a feedback law must be designed to ensure

$$\lim_{t\to\infty} \|y_r(t) - y(t)\| = \lim_{t\to\infty} \|\sigma(t)\| = 0 \tag{9.36}$$

where $\sigma(t) \in \mathbb{R}$ stands for the output error, and $y_r(t)$ is the desired output while providing boundedness of $\dot{q}_2$ and attenuating external disturbances where the reference output $y_r(t)$ is computed online from (9.35).

9.5.1 Case of Study: Inertia Wheel Pendulum

We will illustrate the procedure to find the set of reference trajectories for the inertia wheel pendulum. Let us consider the dynamics of the wheel pendulum in terms of the reference positions and velocities $(q_r, \dot{q}_r)$ without considering the viscous friction force

$$\begin{bmatrix} J_1 & J_2 \\ J_2 & J_2 \end{bmatrix} \begin{bmatrix} \ddot{q}_{1r} \\ \dot{q}_{2r} \end{bmatrix} + \begin{bmatrix} h \sin q_{1r} \\ 0 \end{bmatrix} = \begin{bmatrix} 0 \\ 1 \end{bmatrix} \tau_r. \tag{9.37}$$

We need to find the reference torque $\tau_r \in \mathbb{R}$ to produce a set of desired periodic motion of the underactuated link ($y = q_{1r}$) such that the output has a periodic motion with desired frequency and amplitude. As will be shown later, viscous friction is not required in the above equation since it acts as a damping force thus ensuring the stability of the closed-loop system.

In the results published in [[1, 5, 6]], the self-oscillations were generated in an inertia wheel pendulum using the two relay controller without tracking control. Consequently, the closed-loop system becomes sensitive to disturbances and uncertainties of the model. Now, the proposed framework for trajectory generation under the same methodology and the robust state-feedback tracking controller contributes to avoid sensitivity to external disturbances and unknown dynamics. Here, we mean that the deviation of the frequency and amplitude of the periodic trajectory at the output of the closed-loop structure proposed in [[1, 5, 6]] with respect to the desired ones, depended on the uncertainties of the parameters of the model because formulas to compute the two values of the two-relay controller (c_1 and c_2) depends of the values of the inertia, length of the link, and masses, only; while viscous friction level was not considered as part of the formulas however exists in the system. Now, the proposed scheme is robust with respect to effect of viscous friction and external disturbances which will be rejected using a second-order sliding mode tracking controller.

The inertia wheel pendulum has underactuation degree one and satisfies certain structural property noted in [[18]]. As a result, it is possible to make exact linearization thus achieving local stability of zero dynamics. Following [[18]], let us take

$$\begin{aligned} p_1 &= q_{1r} - \pi + J_1^{-1} J_2 q_{2r} \\ \eta &= J_1 \dot{q}_{1r} + J_2 \dot{q}_{2r} + K p_1 \end{aligned}$$

where $K > 0$ is a constant. It is easy to verify that

$$J_1 \dot{p}_1 = \eta - K p_1$$

while

$$\begin{aligned} \dot{\eta} &= K J_1^{-1} J_2 \dot{q}_{2r} - h \sin(q_{1r}) + K \dot{q}_{1r}, \\ \ddot{\eta} &= -h \cos(q_{1r}) \dot{q}_{1r} - K J_1^{-1} h \sin(q_{1r}), \\ \dddot{\eta} &= R(q_{1r}, \dot{q}_{1r}) + H(q_{1r}) \tau_r \end{aligned}$$

where

$$\begin{aligned} H(q_{1r}) &= \frac{h\cos(q_{1r})}{J_1 - J_2}, \\ R(q_{1r},\dot{q}_{1r}) &= h\left(\dot{q}_{1r}^2 + H(q_{1r})\right)\sin(q_{1r}) - \frac{hK}{J_1}\dot{q}_{1r}\cos(q_{1r}). \end{aligned} \tag{9.38}$$

Hence, we can take

$$\tau_r = H^{-1}(q_{1r})\left(u_r - a_0\eta - a_1\dot{\eta} - a_2\ddot{\eta} - R(q_{1r},\dot{q}_{1r})\right), \tag{9.39}$$

where $H(q_r)$ is nonsingular around the equilibrium point $(q_{1r}^\star, \dot{q}_{1r}^\star) = (\pi, 0)$, a_0, a_1, and a_2 are positive constants. Introducing the new state coordinates $x = (x_1, x_2, x_3) = (\eta, \dot{\eta}, \ddot{\eta})$, we obtain

$$\begin{bmatrix} \dot{x}_1 \\ \dot{x}_2 \\ \dot{x}_3 \end{bmatrix} = \begin{bmatrix} 0 & 1 & 0 \\ 0 & 0 & 1 \\ -a_0 & -a_1 & -a_2 \end{bmatrix} \begin{bmatrix} x_1 \\ x_2 \\ x_3 \end{bmatrix} + \begin{bmatrix} 0 \\ 0 \\ 1 \end{bmatrix} u_r, \tag{9.40}$$

$$\dot{p}_1 = -\frac{K}{J_1}p_1 + \frac{1}{J_1}y_r, \qquad y_r = \begin{bmatrix} 1 & 0 & 0 \end{bmatrix} x. \tag{9.41}$$

The following *two-relay controller* is proposed for the purpose of exciting a periodic motion in (9.40):

$$u_r = -c_1\,\mathrm{sign}(y_r) - c_2\,\mathrm{sign}(\dot{y}_r) \tag{9.42}$$

where c_1 and c_2 are scalars parameters designed such that the scalar-valued function output $y_r(t)$ has a periodic motion with the desired frequency Ω and amplitude A_1. Let us recall that the difference between (9.42) and the second order sliding mode controller given, for example, in [[20]] is that c_1 is not constrained to be positive and greater than c_2.

Let us define the tracking error as:

$$\begin{aligned} \sigma(t) &= q_{1r}(t) - q_1(t) \\ \dot{\tilde{q}}_2(t) &= \dot{q}_{2r}(t) - \dot{q}_2(t). \end{aligned} \tag{9.43}$$

The second-order sliding mode controller can be straightforwardly synthesized from (9.43) obtaining:

$$\begin{aligned} \tau = &-\frac{\Delta}{J_2}\left(\alpha_1\,\mathrm{sign}(\sigma) + \alpha_2\,\mathrm{sign}(\dot{\sigma}) + \beta_1\sigma + \beta_2\dot{\sigma} - \gamma\dot{\tilde{q}}_2\right) \\ &- h\sin(q_{1r} - \sigma) + f_s(\dot{q}_{2r} - \dot{\tilde{q}}_2) - \frac{\Delta}{J_2}\ddot{q}_{1r} \end{aligned} \tag{9.44}$$

where $\Delta = (J_1 - J_2)J_2$. The role of $\gamma\dot{\tilde{q}}_2$ is to avoid that the wheel velocity saturates after a while because the pendulum is influenced by the acceleration of the wheel.

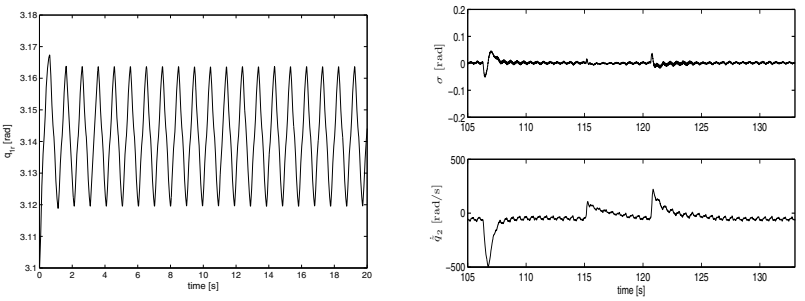

Fig. 9.2 Periodic reference signal at $\Omega = 2\pi$ [rad/s] and $A_1 = 0.07$ generated by the two-relay controller reference model under the parameters $c_1 = 2$, $c_2 = -0.1$, $K = 1 \times 10^{-4}$, $a_0 = 350$, $a_1 = 155$, and $a_2 = 22$ (left). Tracking error of the underactuated link σ under disturbances and perturbed velocity of the disk (right).

Fig. 9.2 shows the trajectory of the reference signal for the reaction wheel pendulum used as reference model. Figure 9.2 also shows the experimental trajectories of the pendulum for the unperturbed and perturbed case, respectively. Details in using quasi-continuous high-order sliding modes is presented by Estrada *et al.* [[14]].

9.6 Comments

Of course, the considered two-relay control algorithm is not the only one that can be used for the purpose of inducing oscillations in dynamical systems. Development of efficient algorithms for purpose of inducing oscillations in mechanical systems, methods of their analysis and design is still an open problem mainly for systems with degree of underactuation higher than one. In fact, the described method just presents a new approach, which is promising in the authors' opinion. In particular, this concerns the use of such simple and efficient methods as the describing function and LPRS methods. In the describing function analysis, sacrificing of exactness of amplitude/frequency computing in favor of simplicity is quite justified by the availability of qualitative results and important conclusions. The LPRS method provides the same functionality even without sacrifice of exactness.

The key feature of the proposed method is that the underactuated system can be considered as a system with unactuated dynamics with respect to the actuated variables. For generation of the self-excited oscillations with desired output amplitude and frequencies, a two relay controller is proposed. A systematic approach for two-relay controller parameter adjustment is proposed. The DF method provides approximate values of the controller parameters for the plants with the low-pass filtering properties. The LPRS gives exact values of the controller parameters for linear plants. The Poincaré maps provides the values of the controller parameters ensuring the existence of the locally orbitally stable periodic motions for an arbitrary

mechanical plant. The effectiveness of the proposed design procedures is supported by experiments carried out on the Furuta pendulum and inertia wheel pendulum from Quanser.

Open questions and problems arising from the above presented results include (a) define conditions of orbital stability for nonlinear plants, (b) generalization of the results for systems that are exactly linearizable, (c) analysis and formulas for bounded control input and bounded outputs systems, (d) define the two-relay controller formulation for underactuated systems with degree of underactuation higher than one.

Acknowledgements. The authors gratefully acknowledge the financial support from CONACYT (Consejo Nacional de Ciencia y Tecnología), grants 132125 and 127575. Programa de Apoyo a Proyectos de Investigación e Innovación Tecnológica (PAPIIT) UNAM, grant 117211.

References

1. Aguilar, L., Boiko, I., Fridman, L., Freidovich, L.: Generating oscillations in inertia wheel pendulum via two relay controller. International Journal of Robust and Nonlinear Control 22, 318–330 (2012)
2. Aguilar, L., Boiko, I., Fridman, L., Iriarte, R.: Generation of periodic motions for underactuated mechanical system via second-order sliding-modes. In: Proc. of the American Control Conference, Minnesota, USA, pp. 5396–5400 (2006)
3. Aguilar, L., Boiko, I., Fridman, L., Iriarte, R.: Output excitation via continuous sliding-modes to generate periodic motion in underactuated systems. In: Proc. of the IEEE Conference on Decision and Control, San Diego, USA, pp. 1629–1634 (2006)
4. Aguilar, L., Boiko, I., Fridman, L., Iriarte, R.: Output excitation via second-order sliding-modes to generate periodic motion for underactuated systems. In: Proc. of the 9th International Workshop on Variable Structure Systems, Alghero, Italy, pp. 359–364 (2006)
5. Aguilar, L., Boiko, I., Fridman, L., Iriarte, R.: Generating self-excited oscillations for underactuated mechanical systems via two relay controller. International Journal of Control 82(9), 1678–1691 (2009)
6. Aguilar, L., Boiko, I., Fridman, L., Iriarte, R.: Generating self-excited oscillations via two-relay controller. IEEE Trans. on Automatic Control 54(2), 416–420 (2009)
7. Aguilar, L., Boiko, I., Iriarte, R., Fridman, L.: Periodic motion of underactuated mechanical systems self-generated by variable structure controllers: design and experiments. In: 2007 European Control Conference, Kos, Greece, pp. 3796–3801 (2007)
8. Atherton, D.: Nonlinear control engineering–Describing Function Analysis and Design. Van Nostrand, Workingham (1975)
9. Berkemeier, M., Fearing, R.: Tracking fast inverted trajectories of the underactuated acrobot. IEEE Transactions on Robotics and Automation 15(4), 740–750 (1999)
10. Boiko, I.: Oscillations and transfer properties of relay servo systems – the locus of a perturbed relay system approach. Automatica 41, 677–683 (2005)
11. Boiko, I.: Discontinuous control systems: Frequency-domain analysis and design. Birkhäuser, Boston (2009)

12. Chevallereau, C., Abba, G., Aoustin, Y., Plestan, E., Canudas-de-Wit, C., Grizzle, J.: Rabbit: A testbed for advanced control theory. IEEE Control Systems Magazine 23(5), 57–79 (2003)
13. Dranga, O., Navy, I.: Stability analysis of feedback controlled resonant DC-DC converter using Poincaré map function. In: IEEE Int. Symposium on Industrial Electronics, Pusan, Korea, pp. 2142–2147 (2001)
14. Estrada, A., Fridman, L.: Exact compensation of unmatched perturbation via quasi-continuous HOSM. In: 47th IEEE Conference on Decision and Control, Cancún, México, pp. 2202–2207 (2008)
15. Fendrich, O.: Describing functions in limit cycles. IEEE Transactions on Automatic Control 37(4), 486–488 (1992)
16. Fridman, L.: An averaging approach to chattering. IEEE Transactions on Automatic Control 46(8), 1260–1265 (2001)
17. Fridman, L.: Slow periodic motion in variable structure systems. International Journal of Systems Science 33(14), 1145–1155 (2002)
18. Grizzle, J., Moog, C., Chevallereau, C.: Nonlinear control of mechanical systems with an unactuated cyclic variable. IEEE Transactions on Automatic Control 50(5), 559–576 (2005)
19. Lai, J.: Power conditioning circuit topologies: Power conversion from low-voltage dc to high-voltage ac for single-phase grid-tie applications. IEEE Ind. Electronics Mag. 3(2), 24–34 (2009)
20. Levant, A.: High-order sliding modes: differentiation and output-feedback control. International Journal of Control 76, 924–941 (2003)
21. Martínez, S., Cortés, J., Bullo, F.: Motion Planning and Control Problems for Underactuated Robot. In: Bicchi, A., Christensen, H.I., Prattichizzo, D. (eds.) Control Problems in Robotics. STAR, vol. 4, pp. 59–74. Springer, Heidelberg (2003)
22. Martínez-Salamero, L., Valderrama-Blavi, H., Giral, R., Alonso, C., Estibals, B., Cid-Pastor, A.: Self-oscillating DC-to-DC switching converters with transformer characteristics. IEEE Transactions on Aerospace and Electronic Systems 41(2), 710–716 (2005)
23. Nakamura, Y., Suzuki, T., Koinuma, M.: Nonlinear behavior and control of a nonholonomic free-joint manipulator. IEEE Transactions on Robotics and Automation 13(6), 853–862 (1997)
24. Orlov, Y., Aguilar, L., Acho, L., Ortiz, A.: Asymptotic harmonic generator and its application to finite time orbital stabilization of a friction pendulum with experimental verification. International Journal of Control 81(2), 227–234 (2008)
25. Orlov, Y., Riachy, S., Floquet, T., Richard, J.: Stabilization of the cart-pendulum system via quasi-homogeneous switched control. In: Proc. of the 2006 Int. Workshop on Variable Structure Systems, Alghero, Italy, pp. 139–142 (2006)
26. Robinett, I.R., Wilson, D.: What is a limit cycle? International Journal of Control 81(12), 1886–1900 (2008)
27. Sanchis, P., Ursua, A., Gubia, E., Marroyo, L.: Buck-boost DC-AC inverter for a new control strategy. In: 35th Annual IEEE Power Electronics Specialist Conference, Aachen, Germany, pp. 3994–3998 (2004)
28. Santiesteban, R., Floquet, T., Orlov, Y., Riachy, S., Richard, J.: Second order sliding mode control for underactuated mechanical system II: orbital stabilization of an inverted pendulum with application to swing up/balancing control. International Journal of Robust Nonlinear Control 18(4–5), 544–556 (2008)

29. Shiriaev, A., Perram, J., Canudas-de-Wit, C.: Constructive tool for orbital stabilization of underactuated nonlinear systems: virtual contraint approach. IEEE Transactions on Automatic Control 50(8), 1164–1176 (2005)
30. Utkin, V., Guldner, J., Shi, J.: Sliding Mode Control in Electromechanical Systems. CRC Press, Boca Raton (1999)
31. Varigonda, S., Georgiou, T.: Dynamics of relay relaxation oscillators. IEEE Transactions on Automatic Control 46(1), 65–77 (2001)
32. Youssef, M., Jain, P.: A novel single stage AC–DC self-oscillating series-parallel resonant converter. IEEE Transactions on Power Electronics 21(6), 1735–1744 (2006)